InP monolithically integrated wavelength selector based on periodic optical filter and optical switch chain

InP monolithically integrated wavelength selector based on periodic optical filter and optical switch chain

Nicola Calabretta*, Ripalta Stabile, Aaron Albores-Mejia, Kevin A. Williams and Harm J. S. Dorren

[1]*COBRA Research Institute, Eindhoven University of Technology, P. O. Box 513, Eindhoven, The Netherlands*
[*]*n.calabretta@tue.nl*

Abstract: We present an InP monolithically integrated wavelength selector that implements a binary search for selecting *N* modulated wavelengths. The wavelength selector filter is realized using log_2N an active Mach-Zehnder interferometer filter and broadband optical gating elements. Nanosecond reconfigurable operation with a spectral-alignment over 3.2nm free spectral range is achieved with an extinction ratio exceeding 25dB. Error-free operation of the wavelength selector for four modulated wavelengths with 2 dB of power penalty is demonstrated.

OCIS codes: (130.7408) Wavelength filtering devices; (200.4740) Optical processing; (060.6719) Switching, packet; (250.5980) Semiconductor optical amplifiers.

References and links

1. N. Amaya, I. Muhammad, G. S. Zervas, R. Nejabati, D. Simeodinou, Y. R. Zhou, and A. Lord, "Experimental demonstration of a gridless multi-granular optical network supporting flexible spectrum switching", in Proc. OFC/NFOEC, San Diego, CA, OMW3 (2011).
2. A. d'Alessandro, D. Donisi, L. De Sio, R. Beccherelli, R. Asquini, R. Caputo, and C. Umeton, "Tunable integrated optical filter made of a glass ion-exchanged waveguide and an electro-optic composite holographic grating," Opt. Express **16**(13), 9254–9260 (2008).
3. S. T. Chu, B. E. Little, V. Van, J. V. Hryniewicz, P. P. Absil, F. G. Johnson, D. Gill, O. King, F. Seiferth, M. Trakalo, and J. Shanton, 'Compact full C-band tunable filters for 50 GHz channel spacing based on high order micro-ring resonators,' OFC 2004, Anaheim, PDP9 (2004).
4. X. Lu, M. Li, R. Samarth, and L. Zheng, "Electro-optic tunable bandpass filter based on long-period-grating-assisted asymmetric waveguide coupling," Opt. Eng. **46**, 405081 (2007).
5. E. J. Norberg, R. S. Guzzon, J. S. Parker, L. A. Johansson, and L. A. Coldren, "Programmable Photonic Microwave Filters Monolithically Integrated in InP–InGaAsP," J. Lightwave Technol. **29**(11), 1611–1619 (2011).
6. E. L. Wooten, R. L. Stone, E. W. Miles, and E. M. Bradley, "Rapidly tunable narrowband wavelength filter using LiNbO3 unbalanced Mach-Zehnder Interferometers," J. Lightwave Technol. **14**(11), 2530–2536 (1996).
7. J. Tae Ahn, S. Park, J. Yun Do, J.-M. Lee, M.-H. Lee, and K. Hon Kim, "Polymer Wavelength Channel Selector Composed of Electrooptic Polymer Switch Array and Two Polymer Arrayed Waveguide Gratings, " Photon. Technol. Lett. **16**, 1567–1570 (2004).
8. S. Khalfallah, B. Martin, J. Decobert, S. Fabre, C. Fortin, P. Peloso, I. Guillemot, J. Le Bris, M. Renaud, A. Goth, A. Dupas, L. Gilbert, and D. Pennincks, "First optical packet switching demonstration with sixteen-channel InP monolithically integrated wavelength selector module," in Proceedings of the ECOC 2001, (2001), pp. 80–81.
9. N. Kikuchi, Y. Shibata, H. Okamoto, Y. Kawaguchi, S. Oku, Y. Kondo, and Y. Tohmori, "Monolithically integrated 100-channel WDM channel selector employing low-crosstalk AWG," IEEE Photon. Technol. Lett. **16**, 2481–2483 (2004).
10. Z. Wang, S.-J. Chang, C.-Y. Ni, and Y. J. Chen, "A high-performance ultracompact optical interleaver based on double-ring assisted Mach–Zehnder interferometer," IEEE Photon. Technol. Lett. **19**, 1072–1704 (2007).
11. R. Stabile, N. Calabretta, H. J. S. Dorren, M. K. Smit, and K. A. Williams, "Reconfigurable Monolithic Wavelength Filter Using Gated Amplifying Mach-Zehnders," IEEE Photonics 2011 Conference (IPC11) Arlington, Virginia, MR4 (2011).
12. E. F. Burmeister, J. P. Mack, H. N. Poulsen, J. Klamkin, L. A. Coldren, D. J. Blumenthal, and J. E. Bowers, "SOA gate array recirculating buffer for optical packet switching," in Proceedings of *OFC 2008*, San Diego, USA, OWe4 (2008).

#155827 - $15.00 USD
Received 3 Oct 2011; accepted 17 Oct 2011; published 29 Nov 2011

1. Introduction

High speed and fast reconfigurable multi-rate and grid-less next generation optical networks are currently investigated to handle the ever increasing growth of the Internet traffic [1]. Fast reconfigurable wavelength selectors (WS) that allow for operation on a large number of wavelength channels, with low cross-talk and low OSNR degradation, and with fast dynamic response (in the order of nanoseconds) are essential sub-systems for implementing reconfigurable WDM core and metro networks, optical packet switched networks, and ultrafast optical signal processing. Compact, low power integrated solutions are essential for the sub-system scalability. Implementations based on different technologies have been demonstrated. Several tunable filter based WSs were investigated in [2–6]. However, high losses [2, 4, 6], low speed tuning [3], and narrowband operation [5] are critical issues. In [6] the high losses prevent practical utilization of the all-polymer WS based on electro-optic polymer switch array between two polymer arrayed waveguide gratings (AWG). Lossless InP monolithically integrated AWGs in combination with optical switches based on semiconductor optical amplifiers (SOAs) were successfully demonstrated and applied to demonstrate fast optical packet switching [7, 8]. However, the number of active components in the WS scales linearly with the number of channels N. In [9], a solution was demonstrated that scales as $2x\sqrt{N}$ for N channels. However, for a large number of channels the number of switches still becomes substantial.

Here we present an InP monolithically integrated WS based on a chain of filters and optical switches that requires only $\log_2 N$ switches to select N wavelengths. The chain of filters and optical switches implements, in the optical domain, a sort of binary search between the input wavelengths. The optical switches are based on SOA technology that guarantees nanosecond speed operation and lossless operation. Wavelength-selection functionality is demonstrated using the integrated SOA gates which are either operated in a zero or high current state. To ensure robust system deployment, fine wavelength alignment is shown by means of current tuning in the active Mach-Zehnder filter element with a near linear dependence of peak wavelength with current. Experimental results show error-free wavelength selection of four 10 Gb/s modulated signals at distinct wavelengths by using two optical switches with a power penalty of less than 2 dB.

2. Principle of operation of the wavelength selector

The WS based on binary search is schematically shown in Fig. 1(a). Half of the incoming channels are selected at each node according to the binary state of the node control. Thus, after the first node there will be N/2 channels remaining, then N/4 channels after the second node, and so on until one channel is univocally selected. The amount of required nodes and controls to select a distinct channel is $\log_2 N$. Without losing generality, Fig. 1a shows as an example the operation of the WS for 8 wavelengths (λ_1,.., λ_8). The WS requires three nodes, which is controlled by a binary control. For control signals ‘1 0 1’ for the three nodes, the WS will select the λ_6. At the first node λ_5,.., λ_8 are selected, at the second node λ_5 and λ_6 are selected, and at the third node λ_6 is selected.

The WS based on binary search algorithm can be effectively implemented in the optical domain as shown in Fig. 1(b). Each of the $\log_2 N$ nodes selects half of the incoming channels by using a periodic filter (PF) and an optical switch. The PF spectrally divides half of the channels to output port 1 (black solid line) and the other half to the output port 2 (red dashed line). The optical switch forwards channels from either port 1 or 2 as instructed by the binary control. Note that the PFs at the i-th node have a free-spectral range $FSR_i = BW_{ch} \times N / 2^i$ with i = 1,…, $\log_2 N$ and BW_{ch} the channel bandwidth. This guarantees that the PF at following node spectrally partitions half of the incoming channels to port 1 and the other half to port 2.

#155827 - $15.00 USD Received 3 Oct 2011; accepted 17 Oct 2011; published 29 Nov 2011

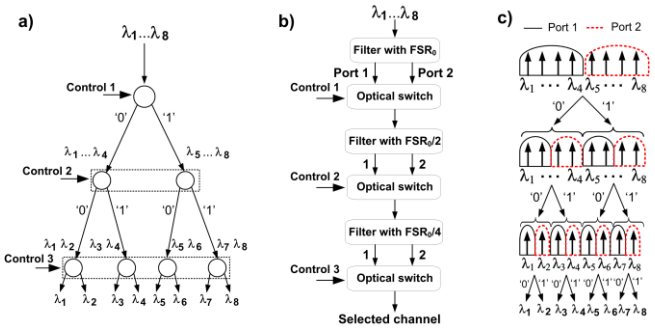

Fig. 1. Operation of (a) the binary search algorithm. (b) The optical WS circuit. (c) Transfer functions of the periodic filter with different free spectral ranges.

Figure 1(b) shows the WS operation with 8 channels. Given '1 0 1' as binary controls, λ_6 is selected by the WS circuit. Indeed, at the first node the PF in combination with the optical switch selects λ_5,.., λ_8. At the second node, the PF with FSR/2 separates the λ_5, λ_6 at port 1 and λ_7, λ_8 at port 2 and the optical switch selects λ_5, λ_6. At the third node, the PF with FSR/4 separates the λ_5 at port 1 and the λ_6 at port 2 and the optical switch selects λ_6. The example in Fig. 1 employed 8 channels and required $3 = \log_2 8$ optical switches and PFs. The operation of the WS can be generalized to N channels by using $\log_2 N$ optical switches and PFs.

As a proof of concept we have fabricated an InP monolithically integrated WS, shown in Fig. 2, capable to select one out of four wavelengths. The PFs were implemented by using MZI filters, and each of the two optical switches consists of two SOAs driven by two complementary electrical signals.

3. Device design and fabrication

The reconfigurable wavelength selector is implemented with a broadband gate stage, a wavelength selective switch stage and a final broadband gate stage monolithically integrated on InP-InGaAsP. Figure 2 shows the schematic layout for the waveguides and the control electrodes. The details at the Mach-Zehnder interferometer (MZI) are enlarged as an inset. The device is fabricated from a four quantum well active InGaAsP/InP epitaxy with a gain spectrum covering the range 1600-1620 nm. A three-step reactive ion etch is performed to define deep, shallow and electrically-isolated waveguides for the required operation. The MZI filter uses deep-etched waveguides to ensure tolerable loss in the 100 μm radius bends. The arrangement can be conveniently concatenated with arbitrary free spectral ranges at each filter stage by changing the differential length in the bends. In this study the filter arm lengths are 500 μm and 272 μm, respectively, and designed to provide a free spectral range of 3.2 nm. The three stages occupy a total area of 1 mm × 4 mm, although this can be readily reduced using shorter amplifier gates. Multimode interference couplers are employed as splitters and combiners. Input and output waveguides are angled at 7° with respect to the facets to suppress reflection. Using a feed-forward filter as the Mach-Zehnder interferometer filter also potentially increases the allowed gain before the occurrence of on-chip oscillation. Nonetheless, here operating currents are restricted to avoid oscillations from the uncoated facets, indicative of high levels of on-chip gain.

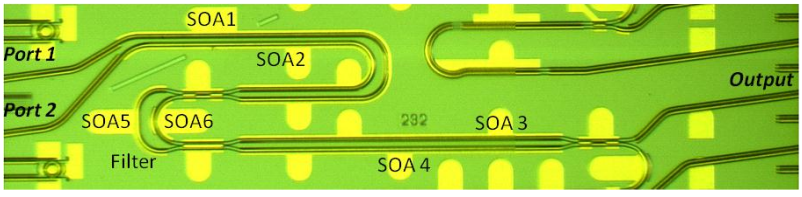

Fig. 2. Microscope image of the fabricated reconfigurable wavelength selector.

#155827 - $15.00 USD
Received 3 Oct 2011; accepted 17 Oct 2011; published 29 Nov 2011

The gold shaded electrodes in Fig. 2 are wire bonded and electronically tuned to study spectral reconfigurability. The first broadband selector stage is operated by complementary biasing of SOA gate 1 and SOA gate 2. The wavelength selective Mach-Zehnder filter stage is operated by biasing the inner short arm with a fixed current near the transparency (20mA), and by varying the outer electrode current. The final broadband switch stage is operated by complementary biasing of SOA gates 3 and 4. The scheme is readily scaled through concatenation.

4. Experimental setup

The experimental set-up employed to demonstrate WS operation with optical packetized signals at different wavelengths is shown in Fig. 3.

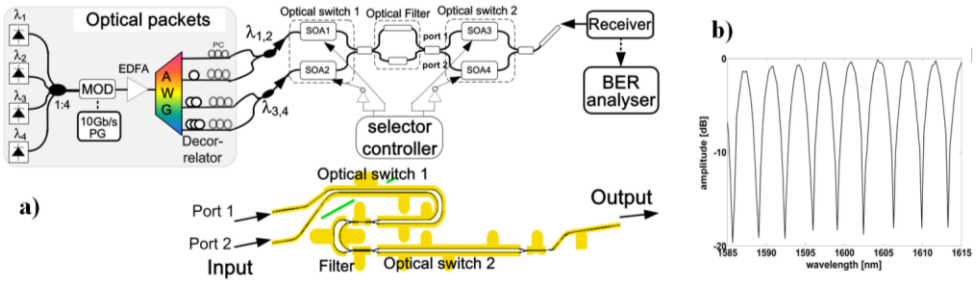

Fig. 3. (a) Experimental set-up. (b) Transfer function of the periodic filter.

First, the static characterization of the WS chip has been performed. Lensed fibers were employed for coupling the light in/out of the chip. DC currents of 110 mA and 114 mA were applied to SOA_1 and SOA_3, while 27.3 mA, 20.2 mA and 3.2 mA and 29.2 mA were applied to the two arms and the two couplers of the active filter, respectively. The SOA at the output of the chip was biased with 35 mA. Figure 3 (b) shows the normalized filter transfer function obtained by scanning an input tunable laser wavelength from 1585 nm to 1615 nm. The transfer function presents a periodicity of 3.2 nm. The −3dB bandwidth of the MZI filter was 1.1nm. The cross-talk between channels spaced by 1.6nm was around −16.5 dB. Cross-talk and flat-top passband can be further improved by using higher order filters [10].

The passbands are registered to the incoming WDM signals. Fine spectral alignment is demonstrated by scanning a tunable laser over the range from 1600 nm to 1607 nm for a signal launched at SOA1 [11]. An optical spectrum analyzer (OSA) measures the optical transmission through the filter device for a range of bias conditions at the longest MZI arm, SOA5 (see Fig. 2). Wavelength is tuned by scanning current from 40.0 to 100.0 mA in Fig. 4(a). The wavelength is changed in the range from 1604.57 to 1609.97 nm covering the overall free spectral range. DC currents of 4.1 mA and 22.8 mA are applied to the two MMI splitters. The shortest MZI arm is biased with a 46.7 mA DC current. SOA1 and SOA3 DC currents are set to 99.4 and 103.1 mA, respectively. The output SOA current is fixed at 46.5 mA and the second last SOA current is 24.5 mA. Figure 4(a) shows the current tuning of high contrast nulls. The extinction ratio increases with the current, and this may be enhanced through the amplified filters themselves. The extinction ratio exceeds 25 dB for 1605.57 wavelength case when increasing the bias current of the long MZI arm from 66.0 to 97.0 mA.

Figure 4(b) shows the continuously programmable fine wavelength tuning: the peak wavelength shifts of 1 nm for almost every 10 mA tuning. In this case the DC current for the shorter arms is fixed at 33.6 mA. SOA1, SOA3 and SOA4 DC currents are changed to 118.3, 72.6 and 96.7 mA, respectively.

Once the WS is spectrally aligned, the static operation of the WS chip was tested by injecting four CW optical signals, λ_1 = 1600.9 nm and λ_2 = 1602.5 nm into port 1, and λ_3 = 1604.1 nm and λ_4 = 1605.7 nm into port 2, respectively (see Fig. 3). The optical switches in

#155827 - $15.00 USD
Received 3 Oct 2011; accepted 17 Oct 2011; published 29 Nov 2011

the WS chip have been electronically switched to select a distinct CW wavelength: when optical switch 1 selects the output port 1 of the MZI filter, only λ_1 or λ_2 is selected when

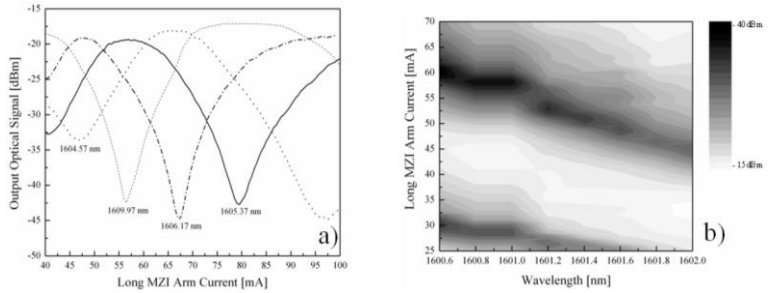

Fig. 4. (a) Output optical signal as a function of the current at the long MZI arm, SOA5, for four input wavelengths covering one free spectral range. (b) Contour map of optical transmission showing the fine wavelength tuning as a function of the current of SOA5.

optical switch 2 selects output port 1 or output port 2 of the MZI filter, respectively. Setting optical switch 1 to select the output port 2 of the MZI filter, only λ_3 or λ_4 is selected when optical switch 2 selects output port 1 or output port 2 of the MZI filter, respectively. The four measured spectra at the chip output for the four combinations are shown in Fig. 5 (a-d). These static results clearly show the WS operation. The measured cross-talk was lower than −16 dB, and the OSNR of the selected CW signals were larger than 30 dB. Scaling the WS operation to a larger number of channels will be limited by the OSNR degradation caused by the accumulated ASE noise of the SOAs in the chain. An OSNR larger than 26 dB after 8 SOA-based recirculation loops was measured in [12]. This indicates that potentially a WS with a chain of 8 passive filters and 8 SOA switch stages is possible enabling selection from 256 modulated wavelengths.

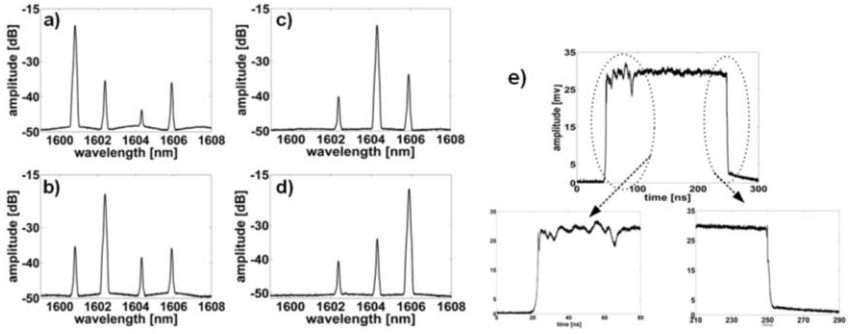

Fig. 5. Optical spectra recorded at the WS output for four different operation of the selector. Selecting (a) λ_1. (b) λ_2. (c) λ_3. (d) λ_4. (e) Time response of the SOA of the optical switch.

We have also investigated the time response of the WS chip. We fed a CW signal into the WS and we applied an electrical pulsed signal with 5 V of amplitude and a rising and falling time of 2 ns to the optical switch. Figure 5 (e) shows the photo-detected output of the WS showing a rise time and fall time of around 4.6 and 3.2 ns (10-90% transitions), respectively. Electrical reflections are seen to lead to a dip in the time resolved gain 46 ns after the turn-on transient. This is expected to be eliminated by implementing high speed drivers in close proximity to the chip.

To investigate the dynamic operation of the WS chip, we generated optical packets at $\lambda_1,\ldots, \lambda_4$ by using an amplitude modulator driven by 10 Gb/s pattern generator with a 2^{11}-1 PRBS interleaved with 512 bits sequence of zeros (see Fig. 6a). This results in a packet guard-time of 51.2 ns, which is sufficient to guarantee the response of the SOA to be flat with respect to the applied control, avoiding the dip 46 ns after turn on. The colored optical packets

#155827 - $15.00 USD Received 3 Oct 2011; accepted 17 Oct 2011; published 29 Nov 2011

were amplified, wavelength demultiplexed and decorrelated, before being fed into the WS chip. Two pairs of modulated signals λ_1, λ_2 and λ_3, λ_4 were fed into the two inputs of the WS, respectively. The optical power of each signal was −2 dBm at the input fiber lens. The output power was −13dBm per channel. Assuming 6 dB/facet coupling losses, the chip losses are compensated by the SOAs. SOA_1, SOA_2, SOA_3, and SOA_4 of the two optical switches were driven by electronic control signals with 5.2 V, 5.1 V, 5.4 V, and 5.8 V, respectively. Note that most of the voltage is dropped across the 39 Ω matching resistor between the 50 Ω controller and the chip. By using a regular current source, the required voltage would be around 1.5 V. Figures 6(b-e) show the control signals appropriately delayed to dynamically select one distinct wavelength at a time. Figures 6 (f-i) report the time-domain traces for each of the four wavelengths at the output of the WS. Those traces clearly show that according to the control pattern only the one optical wavelength packet is selected by the WS. The average extinction ratio was higher than 15 dB.

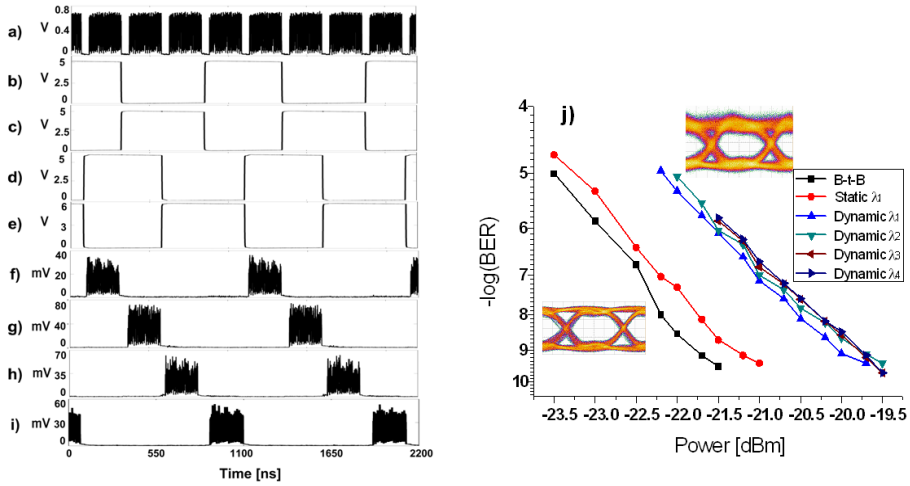

Fig. 6. (a) Input packets. (b-c) Complementary controls applied to SOA1, SOA2 of the optical switch 1. (d-e) Complementary controls applied to SOA3, SOA4 of the optical switch 2. (f-i) WS output traces for the four wavelengths. BER curves of the back-to-back and static selected wavelength at λ_1, and of the dynamic packet selected operation. Inset, eye diagrams of the signal before and after the WS at λ_1.

The eye diagrams measured at the input and output of the WS chip are shown in Fig. 6 (j), respectively. The eye diagram at the WS output is clearly open but it is slightly degraded due to cross-gain modulation in the SOA and noise. The BER curves of the selected packets are reported in Fig. 6 (j). The BER curve in back-to-back configuration is provided as reference. We also report the BER curve in static operation of the WS recorded when only one wavelength (λ_1) is transmitted through the WS. Error-free operation with a power penalty of 0.5 dB was measured. Error-free operation is also obtained for the dynamic selection of the packets at different wavelengths with a power penalty of 1.7- 2.1 dB, which is around 1.2 dB larger than the static case. The penalty is mainly due to cross-gain modulation between the signals and ASE from the SOAs.

5. Conclusions

We have fabricated and demonstrated a new fast InP monolithically integrated WS based on a cascade of periodic filters and optical switches that requires log_2N optical switches for selecting N wavelength signals. The wavelength selector can be spectrally aligned to the incoming WDM signals electronically to select the required wavelength with an extinction ratio exceeding 25 dB at a tuning rate of 0.1nm/mA. Experimental results show error-free wavelength selection of four modulated signals at distinct wavelengths by using two optical switches with a power penalty of less than 2 dB.

#155827 - $15.00 USD Received 3 Oct 2011; accepted 17 Oct 2011; published 29 Nov 2011